

Selenoyl-trifluoroacetone: Synthesis, properties, and complexation ability towards trivalent rare-earth ions

Maxim A. Lutoshkin^{a,b,*}, Ilya V. Taydakov^{c,d}

^a Université de Lyon, Université Claude Bernard Lyon 1, CNRS, IRCELYON, Institut de Recherches sur la Catalyse et l'Environnement de Lyon, Villeurbanne, France

^b Institute of Chemistry and Chemical Technology SB RAS, Federal Research Center "Krasnoyarsk Science Center SB RAS", Krasnoyarsk, Russian Federation

^c P. N. Lebedev Institute of Physics of the Russian Academy of Sciences, Moscow, Russian Federation

^d G.V. Plekhanov Russian University of Economics, 36 Stremyanny Per., 117997 Moscow, Russian Federation

ABSTRACT

The selenium-containing analog of thenoyl-trifluoroacetone has been synthesized and first characterized by UV-visible and NMR-spectroscopies. Synthesis of selenoyltrifluoroacetone was performed by a two-step procedure: acetylation of selenophene and interaction of 2-acetylselenophene with ethyl-trifluoroacetate. The structure of the obtained product has been confirmed using NMR, EI-MS, and elemental analysis. Spectral, acid-base, complexing, and keto-enol parameters were studied under various conditions. Received values of dissociation and protonation constants characterize selenoyltrifluoroacetone as a stronger acid and stronger base than acetylacetone. The aqueous chelation with sixteen rare-earth metals has been studied in acetate and glycine buffer media at I = 0.5 M (NaCl). Values of logK non-monotonically increase from La(III) to Lu(III) and lay within the range of 4.5–11.5 logarithmic units. Most of the determined formation constants were higher than analogous values for thenoyl- and furoyl-trifluoroacetone rare-earth metal complexes. Thermodynamic and spectral parameters were simulated using both DFT and TD-DFT approaches.

1. Introduction

1,3-Dicarbonyl compounds constitute a wide class of bidentate O-donor ligands, which are effective chelation agents. The enormous diversity of the metal-organic frameworks, chelates, and coordination polymers with various supramolecular architectures can be formed by β -diketonate structures [1,2]. These coordination compounds have various potential applications in the different branches of modern technologies: heterogeneous catalysis [3,4], optical [5] and magnetic [6] materials, anticancer drugs [7], and others. Perfluorinated 1,3-dicarbonyl ligands are widely used as extraction and separation agents [8,9]. They have shown high selectivity on various groups of metal ions, especially on Rare-Earth Metals (REMs) [10].

Thenoyl-trifluoroacetone – one of the most universal ligands for separation of REMs(III) and can be used in combination with various organic solvents [11,12]. The synthesis and study of its derivatives and analogous may help to obtain new high-selectivity ligands for the extraction and separation of REMs and other metals. Of particular interest are analogous compounds with chalcogen elements – selenium and tellurium. The presence of selenophene ring in the structure of β -diketonate complexes could improve the spectral and luminescence properties for application in OLEDs (organic light-emitter diodes)

technology [13]. Thermodynamic parameters of selenium-containing ligands are still poorly understood, but their coordination compounds have exhibited considerable diversity of structures [14,15].

In this way, the goal of this work was the synthesis and characterization of 1,3-dicarbonyl ligand, which containing selenophene group and analysis of its chelation capacity with rare-earth metals. To obtain real parameters of complexation, acid-base characteristics were also studied.

2. Experimental

2.1. Synthesis of selenoyl-trifluoroacetone

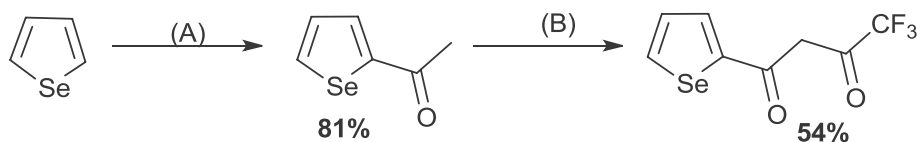
All syntheses were performed under an argon atmosphere using oven-dried (150 °C) glassware. Selenophene (97%) and anhydrous magnesium perchlorate were purchased from Sigma-Aldrich, all other chemicals – from Alfa-Aesar and Acros Organics. Tetrahydrofuran was distilled over sodium/benzophenone in an Argon atmosphere prior to use. The way of the synthesis is shown in Scheme 1.

2.1.1. Synthesis of 2-acetylselenophene

Borosilicate glass vial (30 mL), equipped with PTFE-lined screw cap

* Corresponding author.

E-mail address: maximsfu@yahoo.com (M.A. Lutoshkin).



Scheme 1. Synthesis of 4,4,4-trifluoro-1-selenophen-2-ylbutane-1,3-dione. Reagents and conditions: (A) Ac_2O , $\text{Mg}(\text{ClO}_4)_2$, 90°C , 4 h; (B) NaH , THF, CF_3COOEt , $5-20^\circ\text{C}$.

and a magnetic stirring bar, was charged by 2.71 g (20.6 mmol) of selenophene and 3 mL (3.24 g, 31.7 mmol) of Ac_2O followed by addition of 0.2 g (0.9 mmol, 4 mol %) of $\text{Mg}(\text{ClO}_4)_2$ (caution should be exercised with regard of heating perchlorates in organic solvents [16,17]). The closed vial then was heated at 90°C (bath temperature) with continuous stirring for 4 h and cooled to room temperature. Water (20 mL) was carefully added and the mixture was vigorously stirred for 1 h. An oil was separated, the aqueous phase was extracted 4 times by 15 mL portions of CHCl_3 . The combined organic phase was successively washed by 10 mL of brine, 15 mL of saturated KHCO_3 solution until neutral pH was reached and dried over magnesium sulfate. The solvent was removed on a rotary evaporator and dark oily residue was distilled at 10 torr. 2-Acetylselenophene was afforded as a slightly yellow oil (bp $104-105^\circ\text{C}/10$ torr, lit. $105-106/12$ torr [18]). The yield was 81% (2.97 g). ^1H NMR (300 MHz, CDCl_3): δ 2.45 (s, 3H, CH_3), 7.21 (t, 1H, $J = 4.4$ Hz, C(4)H), 7.78 (d, 1H, $J = 3.3$ Hz, C(3)H), 8.24 (d, 1H, $J = 5.5$ Hz, C(5)H). $^{13}\text{C}\{^1\text{H}\}$ NMR (126 MHz, CDCl_3): δ 26.12 (s, CH_3), 130.72 (s, CH), 134.97 (s, CH), 140.03 (s, CH), 151.46 (s, C(2)), 191.78 (s, C=O). ^{77}Se NMR (95 MHz, CDCl_3): δ , ppm 830.72. Anal. calc. for $\text{C}_6\text{H}_6\text{OSe}$ (173.07): C, 41.64, H, 3.49%. Found: C, 41.27, H, 3.52%. MS (EI, 70 eV): m/z (%) 270(100) $[\text{M}]^+$, 201(69.4) $[\text{M}-\text{CF}_3]^+$, 159(64.7) $[\text{C}_4\text{H}_3\text{SeCO}]^+$, 131(24.0) $[\text{C}_4\text{H}_3\text{Se}]^+$, 69 (75.7) $[\text{CF}_3]^+$.

2.1.2. Synthesis of 4,4,4-trifluoro-1-selenophen-2-ylbutane-1,3-dione

Operations were also performed under the Argon atmosphere. Sodium hydride (60% dispersion in mineral oil, 1.6 g, 40 mmol) was placed in 3-neck round bottom flask and washed 3 times with 20 mL of dry hexane. The last portion of hexane was carefully removed by a glass pipette, and 15 mL of dry THF was added. A solution of 2-acetylselenophene (1.8 g, 10 mmol) and ethyl trifluoroacetate (2.1 g, 1.76 mL, 15 mmol) in 10 mL of THF was slowly added to a vigorously stirred suspension of NaH via dropping funnel. The reaction mixture was stirred until hydrogen evolution ceased (1–2 h), and then left at room temperature for 3 h with slow stirring. Then the dark red suspension was cooled to $+5^\circ\text{C}$ and an excess of NaH was decomposed by slow addition of MeOH (10 mL), followed by the addition of $\text{AcOH-Et}_2\text{O}$ mixture (2.4 mL of glacial AcOH and 10 mL of Et_2O). The yellow solution was evaporated at diminished pressure, the oily residue was mixed with 50 mL of cold water, and pH was adjusted to 4 by HCl . Diketone was extracted by 4 portions of CHCl_3 (30 mL each), combined organic extracts were washed by 10 mL of brine and dried over Na_2SO_4 . Solvents were removed and resulted oil was distilled in the vacuum. The fraction with the boiling interval of $150-152^\circ\text{C}$ at 25 torr was collected. The yield was 1.46 g (54%) of yellow liquid, which solidified upon standing to light a yellow crystalline mass. Mp $30-31^\circ\text{C}$ (lit. $32-33^\circ\text{C}$ [19]). ^1H NMR (300 MHz, CDCl_3): δ , ppm 6.46 (s, 1H, $\text{CH}=\text{C}$), 7.45 (t, 1H, $J = 4.2$ Hz, C(4)H), 8.06 (d, 1H, $J = 4.0$ Hz, C(3)H), 8.52 (d, 1H, $J = 5.6$ Hz, C(5)H), 14.5 (br. s, OH). ^{19}F NMR (282.5 MHz, CDCl_3): δ , ppm -76.45 . $^{13}\text{C}\{^1\text{H}\}$ NMR (126 MHz, CDCl_3): δ , ppm 92.95 (s, $\text{CH}=\text{C}$), 118.76 (q, $J = 280.3$ Hz, CF_3), 131.28 (s, CH), 134.99 (s, CH), 141.79 (t, $J = 59.6$ Hz, CH), 146.63 (s, C(2)), 171.07 (q, $J = 36.4$ Hz, $\text{HO-C}(\text{CF}_3)=$), 183.95 (s, C=O). ^{77}Se NMR (95 MHz, CDCl_3): δ , ppm 844.05. Anal. calc. for $\text{C}_8\text{H}_5\text{F}_3\text{O}_2\text{Se}$ (269.08): C, 35.71, H, 1.87%. Found: C, 35.98, H, 1.92%. MS (EI, 70 eV): m/z (%) 174 (48.5) $[\text{M}]^+$, 159(100) $[\text{M}-\text{CH}_3]^+$, 131 (19.3) $[\text{M}-\text{COCH}_3]^+$, 105 (19.4) $[\text{C}_5\text{H}_3\text{Se}-\text{C}_2\text{H}_2]^+$, 43 (23.7) $[\text{CH}_3\text{CO}]^+$.

2.2. Apparatus and procedure

NMR spectra were recorded on Bruker AM300 (^1H and ^{19}F spectra) or on Bruker DRX500 (^{13}C and ^{77}Se spectra) instruments, operated at 300.13, 282.40, 125.76, and 95.36 MHz respectively. The measurements were conducted using the residual signals of the deuterated solvent ($^1\text{H} - 7.16$ ppm, $^{13}\text{C} - 77.16$ ppm). The ^{19}F and ^{77}Se NMR chemical shifts were referenced to external CFCl_3 and Me_2Se standards respectively. Electronic impact ionization mass spectra (EI-MS) were recorded on a Thermo DSQ II instrument operating in direct insert mode. Elemental analyses were performed on a PE 2400 Series CHNS/O Elemental Analyser (PerkinElmer). All NMR and EI-MS spectra are contained in Electronic Supplementary Information. The UV-Vis spectra were measured with the Leki SS2109-UV scanning spectrophotometer (Leki Instruments, Finland) using 1 cm quartz cells. Cell thermostating (± 0.1 K) was performed with the Haake K15 thermostat connected to the Haake DC10 controller. The absorbance of process solutions was measured within 220–500 nm. All UV-Vis measurements were performed at 298 ± 0.1 K.

2.3. Reagents

All chemicals were of analytical grade: $\text{LnCl}_3 \cdot 6\text{H}_2\text{O}$ ($\text{Ln} = \text{Y}, \text{Sc}, \text{La}, \text{Ce}, \text{Pr}, \text{Nd}, \text{Sm}, \text{Eu}, \text{Gd}, \text{Tb}, \text{Dy}, \text{Ho}, \text{Er}, \text{Tm}, \text{Yb}, \text{Lu}$), HCl , NaCl , CH_3COOH , CH_3COONa , Glycine, Citric acid, $\text{Na}_2\text{HPO}_4 \cdot 12\text{H}_2\text{O}$, Tris (tris (hydroxymethyl) aminomethane). All lanthanide chlorides stock solutions were obtained by dissolving in distilled water. Concentrations of stock solutions of lanthanides have been determined by complexometric titration with disodium EDTA. Buffer solutions within the pH range from 1.80 to 3.60 were prepared with glycine and HCl , from 3.60 to 5.60 with CH_3COOH and CH_3COONa , and from 7.00 to 8.00 with Tris and HCl . Citric buffer (citric acid + Na_2HPO_4 , pH from 3.60 to 7.00) was used for the determination of dissociation constants. The concentration of HCl was determined by means of titration with a standardized solution of Na_2CO_3 . The pH meter “Mettler Toledo F20” has been applied for the determination of pH. Interaction between components of buffers used and studied ligand has not been detected.

Sodium chloride was used as a background electrolyte (the formation of chloride complexes of metals can be ignored under such condition [20]). To maintain the accurate value of ionic strength, the concentrations of other ions (buffer components and metal salts) were taking into account. The total value of ionic strength in each sample was 0.50 ± 0.03 M. The ligand was dilute in the selected sample from water-ethanol solution (1:1 vol). The concentration of ethanol did not exceed 2% in the final solution.

2.4. UV-vis measurements

The dissociation constants (K_a) were calculated with the following equations [21]:

$$A_i = \frac{C_{HL}(\epsilon_L \cdot K_a + \epsilon_{HL}[H^+])}{K_a + [H^+]}, K_a = \frac{[L^-][H^+]}{[HL]}, \quad (1)$$

with the Henderson-Hasselbach equation [22]:

$$\text{pH} = \text{p}K_a + \log(\text{IR}); \text{IR} = \frac{A_i - A_{HL}}{A_L - A_i}, \quad (2)$$

where IR – ionization ratio. The non-linear Cox–Yates method [23] based on the excess acidity function χ [24] was applied to determine the protonation constant (K_H) in highly acidic media (m^* -solvation coefficient):

$$A_i = \frac{A_{HL} - A_{H_2L^+}}{1 + \left(\frac{C_{H^+}}{K_H}\right)10^{(m^*\chi)}} + A_{H_2L^+}, K_H = \frac{[HL][H^+]}{[H_2L^+]} \quad (3)$$

where A_i , A_{HL} (ϵ_{HL}), $A_{H_2L^+}$ ($\epsilon_{H_2L^+}$), and A_L (ϵ_L) are the optical density and molar extinction coefficients of the process solution, the neutral ligands, and its conjugate acid or base, respectively.

The conditional stability constants were calculated by Eqs. 4–6 [25]:

$$K' = \frac{[ML]}{[M][HL]} \quad (4)$$

$$A_i = \epsilon_{HL}(C_{HL} - [ML]) + \epsilon_M(C_M - [ML]) + \epsilon_{ML}[ML], \quad (5)$$

$$[ML] = \frac{1}{2} \left[\left(\frac{1}{K'} + C_{HL} + C_M \right) - \sqrt{\left(\frac{1}{K'} + C_{HL} + C_M \right)^2 - 4C_{HL}C_M} \right], \quad (6)$$

where A_i is an absorbance at a given wavelength, C_M and C_{HL} were analytical concentrations of metal and ligand, respectively. K' – conditional stability constant. The ϵ_i ($i = M, HL, ML$) is a value of molar extinction coefficient at single wavelength. The optimal values for K' , K_a , K_H , and extinctions were found from the least squares analysis [26] ($K_i = K', K_a$ or K_H):

$$\sum_{i=1}^n (A_i^{exp} - A_i^{calc})^2 \xrightarrow{K_i, \epsilon_i} \text{minimum} \quad (7)$$

For all estimations the coefficient of determination (R^2) was at least 0.97. The “ \pm ” values represent confidence limits ($P = 0.95$) throughout the article. Values of absorbance at single wavelength are contained in [Supporting Information](#). Calculations of all equilibrium constants and molar extinction coefficients were carried out using Wolfram Mathematica software package [27]. All raw spectral data are given in [Electronic Supplementary Information](#) (Tables S1–S8).

2.5. *Ab initio* study

Quantum-chemical computations were performed using the GAMESS US [28] program package on the cluster MVS-1000 M of the Institute of computational modeling SB RAS. All theoretical calculations were performed with a temperature of 298 K. Geometry optimization was performed by density functional theory (DFT) with PBE0 [29] functional under Grimme’s empirical correction [30], B3LYP [31], BLYP [32], M06, M06-2X, M06-HF, M11-L [33], and revTPSS [34]. The full-electron cc-pVDZ [35] and Def2-TZVP [36] basis set functions were applied for C, O, H, F, and Sc atoms. For Y, La, and Lu atoms CRENBL ECP pseudopotential [37] has been used. The free Gibbs energy of reactions ($\Delta \Delta G^{solv.}$) has been calculated using gas-phase energy (ΔG^{gas}), solvation free energy (ΔG^{aq}), and zero-point energy correction (ΔE^{ZPE}) [38]:

$$\log K^{calc} = -\Delta \Delta G^{solv.}/(2.303RT) \quad (8)$$

Table 1

Extinction coefficients of the maximum absorption wavelengths for various forms of selenoyl-trifluoroacetone and acid-base parameters.

| I, M (NaCl) | 0.25 | 0.50 | 1.00 |
|---|-----------------|-----------------|-----------------|
| pK_a | 6.32 ± 0.03 | 6.40 ± 0.05 | 6.50 ± 0.05 |
| $\log \epsilon^{279}(\text{neutral}) \pm 0.01$ | 4.04 | 4.03 | 4.04 |
| $\log \epsilon^{343}(\text{anion}) \pm 0.01$ | 4.26 | 4.27 | 4.27 |
| $\log \epsilon^{346}(\text{protonated}) \pm 0.01$ | 3.53 | | |
| $-pK_H \pm 0.03$ | −1.85 | | |
| m^* (solvation coefficient) ± 0.05 | 0.45 | | |

$$\Delta \Delta G^{solv.} = \Delta G^{gas} + \Delta G^{aq} + \Delta E^{ZPE} + E^{corr.} \quad (9)$$

$$E^{corr.} = -RT \ln([H_2O]) = -9.964 \text{ kJ/mol.} \quad (10)$$

here, $E^{corr.}$ is a term of free energy change associated with moving a solvent from a standard-state solution phase concentration of 1 M to a standard state of the pure liquid, 55.34 M [39]. Values of $G^{gas}(H^+)$ and $\Delta G^{solv.}(H^+)$ for proton (−26.28 and −1108.27 kJ·mol^{−1}, respectively) have been taken from the previous research [40]. The solvent effects were evaluated using the SMD solvation model [41].

UV–Vis absorption maximum wavelengths of complex species were reproduced from the vertical excitation energies for the first 12 singlet excited states by Time-Dependent Density Functional Theory (TD-DFT) [42].

3. Results and discussion

3.1. Characterization

In contrast with thiophene, electrophilic acylation of selenophene is a much less studied process. Nevertheless, both heterocycles have alike chemical properties, and consequently can be acylated under similar conditions. Several reagents were used previously for the preparation of 2-acetylselenophene, e.g. AcCl-AlCl_3 in CH_2Cl_2 at −15 °C [43,44], $\text{Ac}_2\text{O-H}_3\text{PO}_4$ [45], $\text{Ac}_2\text{O-SnCl}_4$ [46], but the yield of the ketone in all cases was moderate (less than 55%). Since selenophene is expensive, it would be desirable to develop a more efficient synthetic protocol. As it was found by Dorofenko et al. [47], perchloric acid or magnesium perchlorate can be used as very efficient catalysts in the acylation of thiophene by anhydrides of carboxylic acids. We have modified this method for the preparation of 2-acetylselenophene. It can be used on the semi-micro scale, as it was described in the experimental part. The target compounds have been obtained in high (more than 81% after distillation) isolated yield, and the work-up of the reaction mixture was very simple.

Both anhydrous or hydrated $\text{Mg}(\text{ClO}_4)_2$ can be used with the same efficiency, so long as an excess of anhydride was used. The method is safe because only 2–4 mol % of the catalyst is required. Note that mixtures of organic substances with perchlorates are considered to be potentially explosive and should be treated accordingly. Diketones bearing selenophene moiety are still poorly explored up to date. Apparently, the simplest diketone of this type (4,4,4-trifluoro-1-selenophen-2-ylbutane-1,3-dione, Se-CF_3) was first obtained (without a detailed analysis) by Yur’ev et al. by NaNH_2 mediated Claisen-type condensation of CF_3COOEt and 2-acetylselenophene [19].

Although the yield of the desired diketone was around 70 %, sodium amide is a hazardous, non-stable, and heavy-handled reagent. We have investigated previously [48] condensation of 2-acetylthiophenes with esters of perfluorinated carboxylic acids in the presence of different bases (NaH , NaOEt , or NaOMe). Here we have adapted this method for preparation of 4,4,4-trifluoro-1-selenophen-2-ylbutane-1,3-dione. The 3–4-fold molar excess of NaH is mandatory to achieve a high and reproducible yield of diketone. Although the yield of diketone by the described method is lower, the utilization of NaH instead of NaNH_2 is much more convenient. THF is the solvent of choice for this synthesis because sodium diketonate is soluble in it and the reaction proceeds in a homogeneous solution. The isolation of diketone is simple – vacuum distillation is sufficient and purification via precipitation of copper chelate is not needed. Analytically pure samples can be obtained by additional recrystallization of the distilled compound from MeOH but this procedure leads to significant yield losses.

3.2. Acid-base properties

1,3-Diketones exhibit acid-base properties [49,50]. To determine parameters of these properties, Se-CF_3 was studied

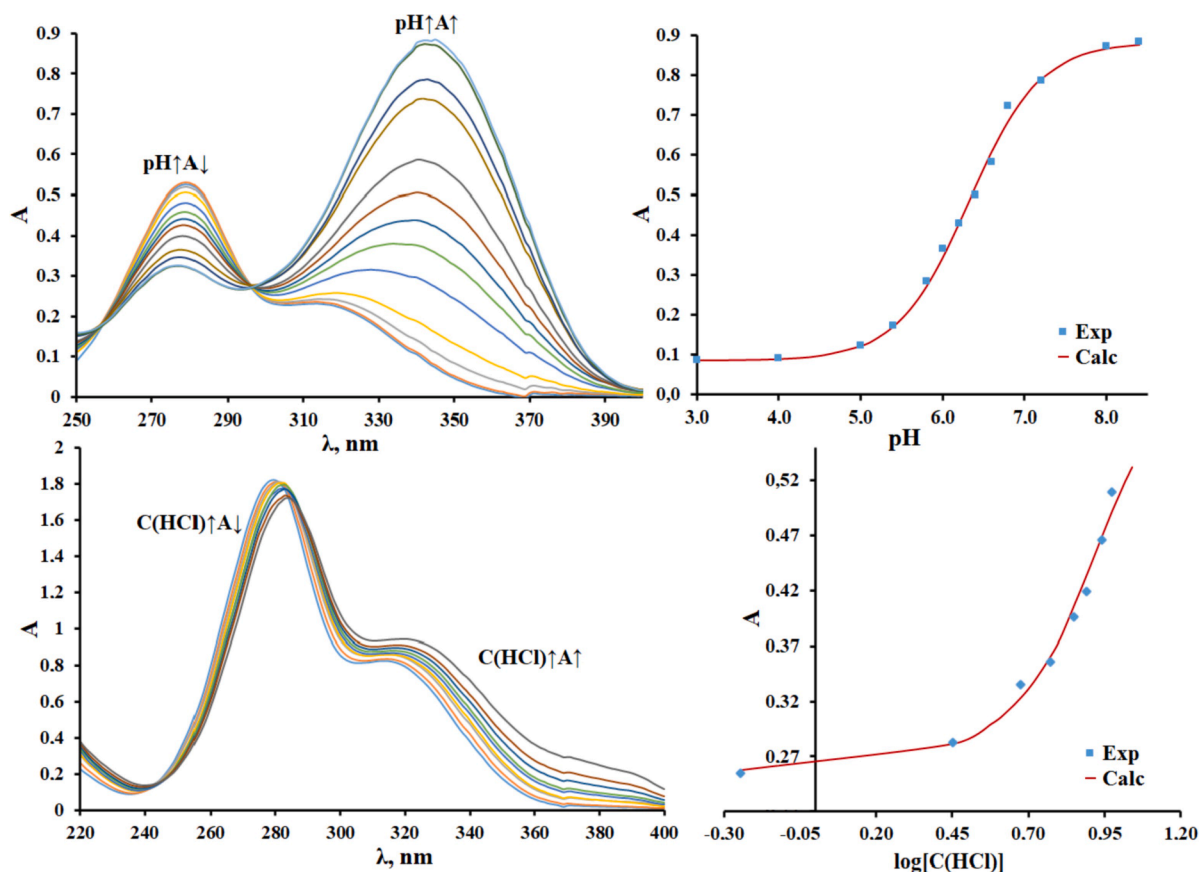


Fig. 1. UV-visible spectra (left) and absorption at single wavelength (right) of selenoyl-trifluoroacetone in pH media (top, $C(\text{Se-CF}_3) = 4.83 \cdot 10^{-5}$ M, $I = 0.25$ M, $\lambda = 343$ nm) and in concentrated HCl (bottom, $C(\text{Se-CF}_3) = 1.74 \cdot 10^{-4}$ M, $\lambda = 346$ nm).

spectrophotometrically in various media. Dissociation processes were studied using glycine-HCl, citric-phosphate, and TRIS-HCl buffers in the pH 3.0–8.4 region. Protonation of selenoyl-trifluoroacetone was conducted in hydrochloric acid solutions, at concentrations of HCl more than 3 M.

Optical and acid-base characteristics of the studied ligand are given in Table 1. Spectra of selenoyl-trifluoroacetone at different pH values are depicted in Fig. 1. Relationships $\log I/R$ -pH (eq. (2)) are contained in supporting information (Fig. S1) and demonstrate that one proton dissociates in the studied region of pH.

The dissociation constant (pK_a) lies within the range 6.32–6.50 logarithmic units and slightly decreases with increases in ionic strength.

The value of pK_a for thenoyl-trifluoroacetone is 6.20 ($I = 0.50$ M) [51], which lines up almost precisely with the value obtained for selenoyl-trifluoroacetone at $I = 0.25$ M. Both of these ligands are stronger acid than acetylacetone ($pK_a = 8.83$ [52]). The similarity of the acidic properties of thenoyl- and selenoyl-trifluoroacetone and their difference from acetylacetone demonstrates the pronounced induction effects of the $-\text{CF}_3$ group.

Base properties of Se-CF_3 characterized by the value of the protonation constant $-pK_H = 1.85 \pm 0.03$. The value obtained suggests that the protonation of Se-CF_3 takes place at HCl concentration of more than 7 M. The studied ligand contains two potential centers of protonation: selenophen- and β -dicarbonyl-group. The solvation coefficient (m^* from eq.

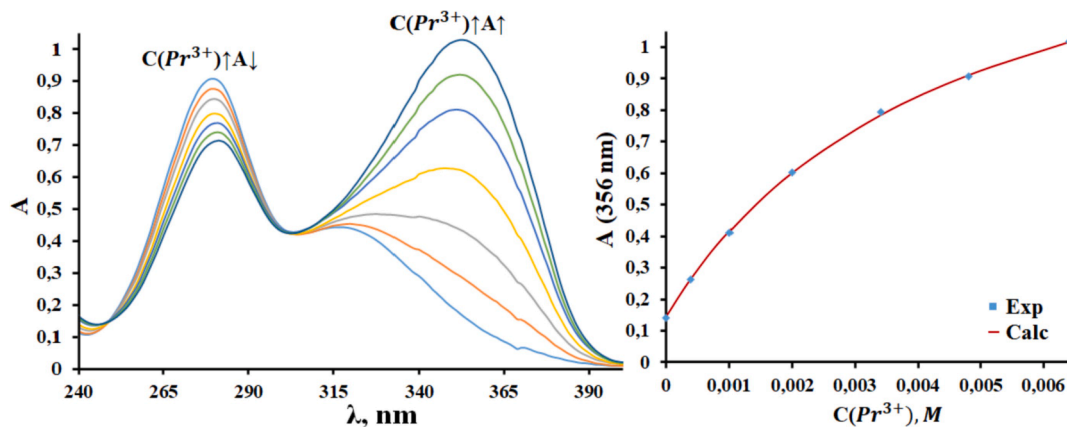


Fig. 2. Spectra of selenoyl-trifluoroacetone under various Praseodymium (III) concentration (top) and absorption at single wavelength as a function of $C(\text{Pr}^{3+})$ – bottom; $C(\text{Se-CF}_3) = 6.19 \cdot 10^{-5}$ M, $\text{pH} = 5.4$, $I = 0.50$ M (NaCl).

Table 2

Conditional (K') and “true” (K) stability constants for selenoyl-trifluoroacetone-REMs(III) systems.

| Metal | pH \pm 0.01 | $\log K' \pm 0.005$ | $\log \epsilon$ (356 nm) \pm 0.01 | $\log K \pm 0.05$ |
|-------|---------------|---------------------|-------------------------------------|-------------------|
| Sc | 3.60 | 2.240 | 4.55 | 11.49 \pm 0.07 |
| Y | 5.00 | 2.492 | 4.34 | 5.61 |
| La | 5.40 | 2.302 | 4.22 | 4.87 |
| Ce | 5.40 | 2.397 | 4.26 | 4.78 |
| Pr | 5.40 | 2.364 | 4.27 | 4.99 |
| Nd | 5.40 | 2.304 | 4.29 | 4.73 |
| Sm | 5.00 | 2.148 | 4.29 | 5.55 |
| | 5.20 | 2.334 | 4.30 | 5.55 |
| | 5.40 | 2.407 | 4.29 | 5.44 |
| Eu | 5.40 | 2.493 | 4.27 | 5.04 |
| Gd | 5.00 | 2.211 | 4.31 | 4.95 |
| | 5.20 | 2.361 | 4.33 | 4.92 |
| | 5.40 | 2.490 | 4.30 | 4.86 |
| Tb | 5.40 | 2.642 | 4.31 | 4.54 |
| Dy | 5.40 | 2.718 | 4.32 | 5.50 |
| Ho | 5.20 | 2.669 | 4.32 | 5.42 |
| Er | 5.20 | 2.741 | 4.34 | 5.49 |
| Tm | 5.00 | 2.647 | 4.33 | 5.40 |
| Yb | 5.20 | 2.819 | 4.34 | 5.64 |
| Lu | 5.00 | 2.681 | 4.31 | 5.50 |

(3) – an important indicator of the mechanism of protonation – is equal to 0.45, which corresponds to coordination through the β -diketonate group [51]. The received value of pK_H is close to the analogous parameters for thenoyltrifluoroacetone derivatives with $-C_2F_5$ and $-C_3F_7$ groups ($-pK_H = 2.15$ – 2.40 [49]).

3.3. Study of complexation with REMs

The molar series method was used for the study of chelation processes between Se- CF_3 and rare-earth metals. Small ligand concentration (4.8 – 8.7×10^{-5} M), pH, and ionic strength ($I = 0.5$ M, NaCl) were invariant for each series. Metal concentration was the variable parameter ($C_M \gg C_L$). Study of complexation was performed in the pH 5.0–5.4 region (selenoyl-trifluoroacetone exists in the neutral form at this acidity). All these factors have contributed to the formation of 1:1 monocomplex species. Typical spectra of the suited ligand under various REMs $^{3+}$ concentrations are depicted in Fig. 2.

Values of conditional stability constants are given in Table 1. Several aspects demonstrate the formation of the ML complex only. Isobestic points show the presence of two absorption species: initial ligand and formed complex. Absorption maximum wavelength on the ΔA - λ curves (Fig. S2, example for Gd^{3+}) remains invariant at various metal

concentrations and pH, indicating a lack of polynuclear complexes. The value of ΔA depends only on metal concentrations and a set of spectral data can be effectively modeling only by the 1:1 complex formation model (eq. 4–6).

Some systems (Sm^{3+} - and Gd^{3+} -selenoyltrifluoroacetone) were studied under several values of pH (5.0–5.4). Both systems demonstrate the linear dependency between conditional stability constants and pH, but the slope coefficient deviates from 1 (0.65–0.70). This is related to the side reactions: interaction of REMs(III) ions with acetate ions, hydrolysis, and dissociation of the ligand. To account for background reactions, following equations were used [21]:

$$K = \alpha_M \alpha_L K' \quad (11)$$

$$\alpha_M = 1 + \sum \beta_n [L]^n, \quad (12)$$

$$\alpha_L = 1 + \sum K_H [H^+]. \quad (13)$$

In equations (11)–(13), K_H is $1/K_a$ of a ligand (determined above), K' and β_n are conditional and cumulative stability constants of the side reactions, respectively. The stability constants of glycine-[53], acetate-[54–56], and hydroxo-complexes [57] were used for calculating α_M and α_L coefficients (Table S9). K is the “true” formation constant, which does not depend on the effects of media (pH, side reactions) and depends only on temperature and ionic strength. “True” stability constants are set out in Table 2.

Values of $\log K$ lay within a range of 4.5–11.5. The maximum and minimum formation constant has been observed for Sc^{3+} and Tb^{3+} , respectively. It is useful to compare obtained parameters with analogous complexes of thenoyl- and furoyl-trifluoroacetone (Fig. 3-A [48]): formation constants for complexes of Y(III), La(III), and Sm(III) are maximum for Se- CF_3 . In contrast, the stability of Tb(III), Tm(III), and Lu(III) complexes are markedly lower than for O- and S-containing trifluoroacetones.

Overall, the change of chalcogen atoms in the C_4H_4X -group ($X = O, S, \text{ or } Se$) has a limited effect on the chelation capacity of the ligand. Absolute values of formation constant (K) for considered ligands differ by 1.1–3.7 times from each other, but their logarithmic values have similar magnitudes. For each of C_4H_4X -($C(=O)$ - CH_2 - $C(=O)$)- CF_3 diketones, we can see the characteristic trend: $\log K$ - M^{3+} curves have the zigzag shape. Fig. 4 (left) demonstrate the $\log K$ - M^{3+} curve for studied systems. The stability of complexes decreases in the series $Yb < Sm = Dy = Er = Lu < Ho = Tm < Eu = Pr < Gd < Ce < Nd < Tb$ for lanthanide, and $Sc > Y > La$ for other rare-earth metals. Among the lanthanides, two triads (Nd-Sm-Eu and Gd-Tb-Dy) form local maximum and minimum,

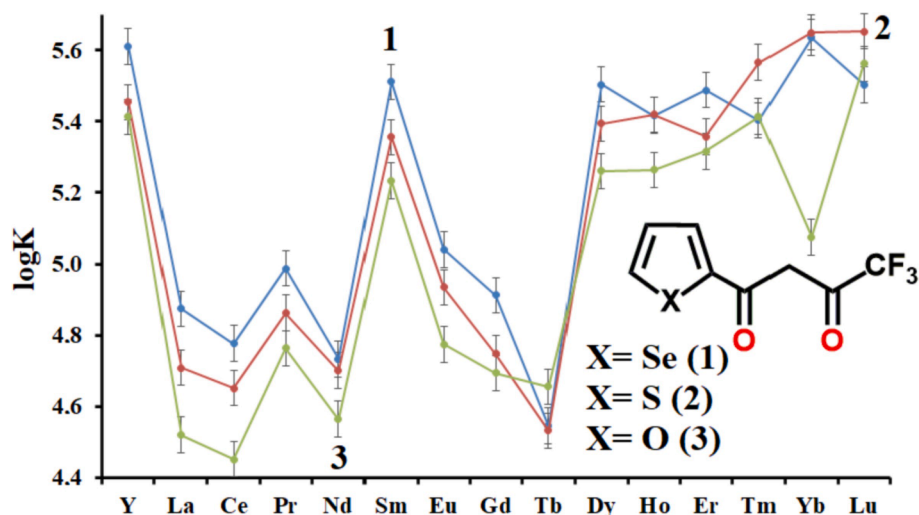


Fig. 3. $\log K$ values for thenoyl-, furoyl-, and selenoyl-trifluoroacetones.

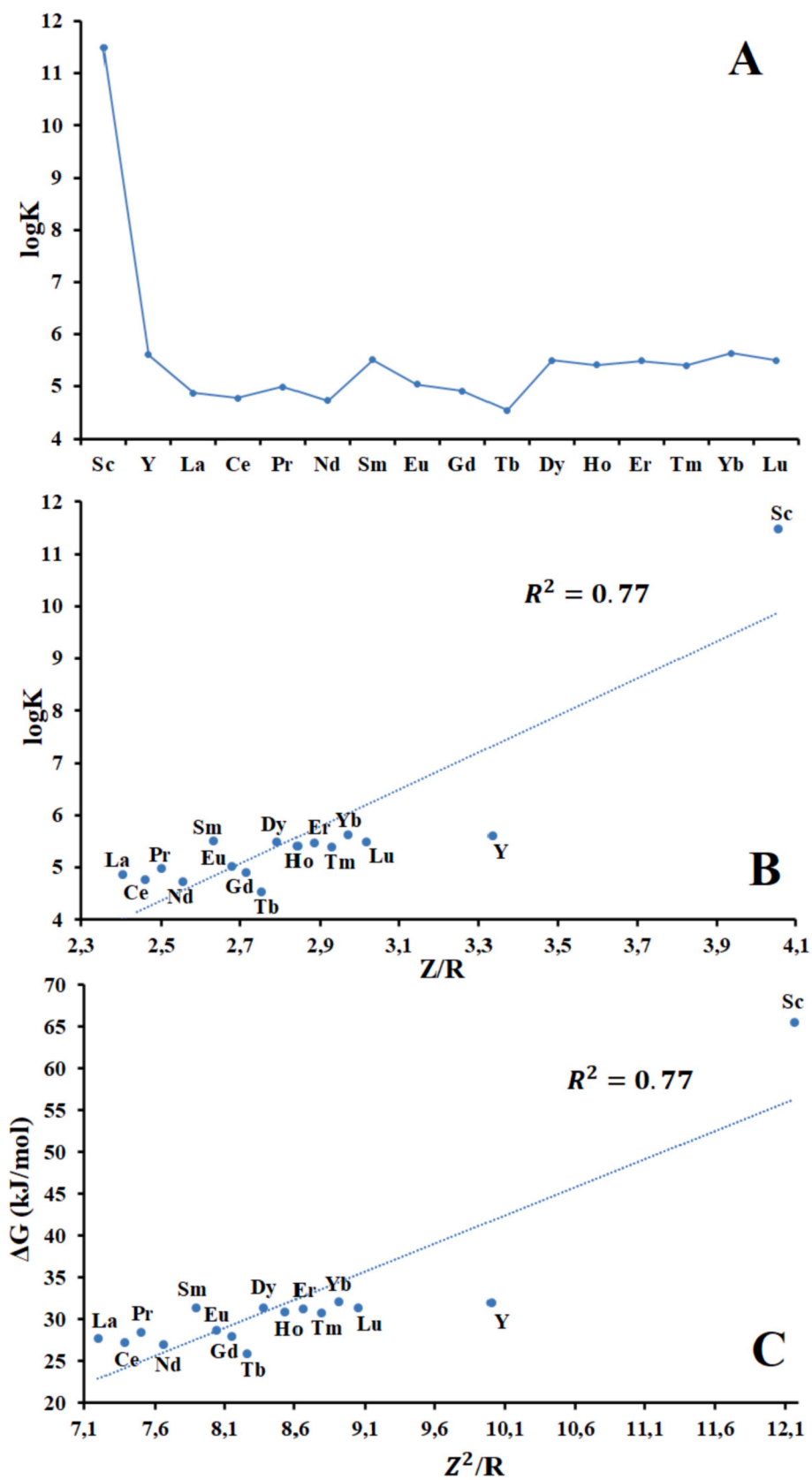


Fig. 4. Relationships logK-REMs (A), logK-Z/R (B), and ΔG- Z²/R (C) distribution.

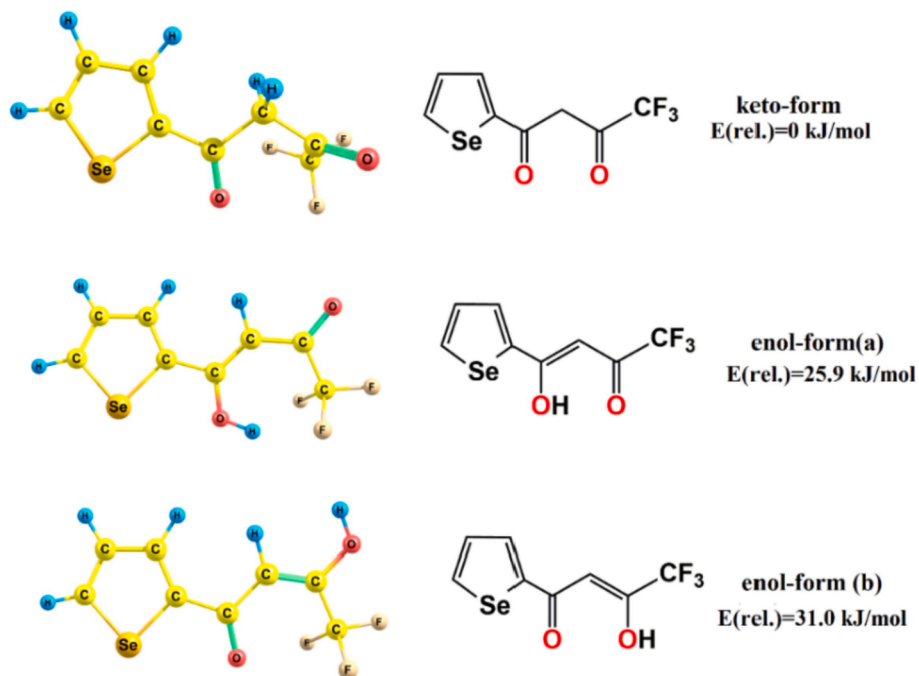


Fig. 5. Structures and parameters of the keto-enol equilibrium.

respectively. Values for stability constants for heavy lanthanides (from Dy to Lu) are almost equal.

Due to the observed behavior is quite hard to explain, we present here the empirical data with the discussion within the first-order approximation. Analysis of the link between thermodynamic and electrostatic parameters can help to understand the nature of formed complexes (Fig. 4, B) [58]. The relationship between formation constants and ionic potential (z/r , where z -charge of metal ion (+3), r -ionic radius [59]) demonstrates a linear correlation and a clear division between three groups: La-Nd, Sm-Tb, and Dy-Lu. For each of these groups, the character of Z/R -logK correlation is different. The gradual increase in the stability constants with an increase in the ionic potential corresponds to the electrostatic model of interaction [60]. The ΔG - Z^2/R graph (Fig. 4, C) shows that the free Gibbs energy of the chelation process is correlated with electrostatic dissipative (Z^2/R). Since Z^2/R can be assigned to a molar Gibbs function of solvation (the change in energy of the electric field [61]), this correlation also demonstrates the

contribution of Coulomb interaction.

For the first group of metals (La^{3+} , Ce^{3+} , Pr^{3+} , and Nd^{3+}), a weak correlation is observed: formation constants non-monotonically increase with ionic potential. The second group demonstrates the lack of relationship between logK and z/r . Formation constants for this group are decreased from Sm^{3+} to Tb^{3+} . A similar pattern was found for other CF_3 -diketones [51]. These four metals have the highest spin among rare-earth metals (Sm^{3+} ($^6\text{H}_{5/2}$; spin 5/2), Eu^{3+} ($^7\text{F}_0$; spin 3), Gd^{3+} ($^8\text{S}_{7/2}$; spin 7/2), Tb^{3+} ($^7\text{F}_6$; spin 3)). Probably, the effect of the lack of electrostatic dependency may be related with spin-orbital interaction i.e. with relativistic effects.

The group of heavy lanthanides (Dy-Lu) show the linear dependency, and for these metals (except Lu^{3+}) stability constants to slowly increase with z/r . As it can be seen above, the considerable variation of the Coulomb interaction contributes exists in the various groups of lanthanides complexes with selenoyl-trifluoroacetone. Similar patterns are presented to a lesser degree for other β -diketones [51].

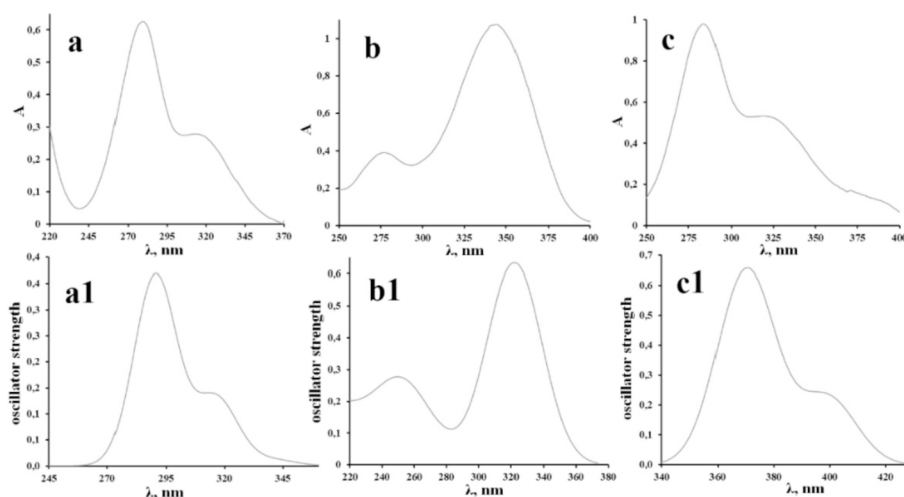
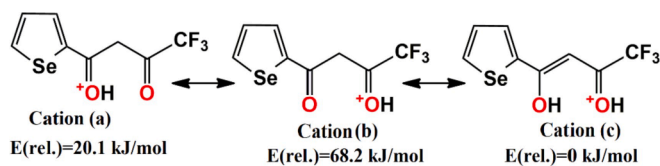


Fig. 6. Experimental (a, b, c) and calculated (a1, b1, c1) absorption spectra; Neutral (a1, a), anionic (b, b1), and protonated (c, c1) form; Bandwidth on $\frac{1}{2}$ weight – 25.

Scheme 2. Tautomerism for protonated form of Se-CF₃.

3.4. DFT calculations

Keto-enol tautomerism is the characteristic process for β -diketones in aqueous solutions. These processes are not always an equilibrium between keto- and enol-form. Thenoyl-trifluoroacetone exists in 1,3-dihydroxy form in ethanol-aqueous media [57]. For other diketones, tautomerism has also apparently included several complicated forms. The analysis of such systems is a difficult case for NMR since perfluorinated β -diketones have low solubility in water. Study in the water-organic solvent leads to the shift of the keto-enol equilibrium due to a reduced dielectric constant of the media.

Quantum-chemical simulations may be effective in this case. Fig. 5 demonstrates possible tautomeric forms of Se-CF₃ and their calculated relative energies. For most diketones, analogous estimates suggest that the enol-form is the most stable isomer [49,50]. In the case of selenoyl-trifluoroacetone, ketone has the lowest energy.

Theoretical spectra (Fig. 6 - a and a1) and positions of wavelength of maximum absorbance for keto-form are close to experimental parameters. Thus, the structure of selenoyl-trifluoroacetone can be simulated by keto-form (Fig. 5, above). The protonated form of Se-CF₃ can also exist in several forms (Scheme 2). For the same reason, the structure of the cation can be approximated by protonated enol-form. In addition, used method (PBE0/SMD) also demonstrate the applicability for calculating of spectral parameters for other β -diketones [51].

Table S10 contains wavelengths of maximum absorbance for various forms estimated by using nine density functionals. M06-L and PBE0 demonstrate a good correlation with experimental parameters for neutral and anionic forms, respectively. Theoretical values for protonated form have a significant difference with observed parameters.

However, the first peak of this form (284 nm) can be reproduced within ± 10 –15 nm by the use of most of the tested functionals. Visualized spectra of various forms are shown in Fig. 6 (revTPSS functional). Acid-base properties were computed using a thermodynamic cycle (Scheme 3 [51]).

In the previous works [46], was shown the effectivity of cc-pVDZ and Def2-TZVP basis set functions for modeling of dissociation and protonation processes, respectively. Here, we use the same computational protocol. Table 3 demonstrates that this approach is justified. Disagreement between theoretical and experimental values of pK_a for M06, M06-2X, and BLYP density functionals does not exceed 0.2 logarithmic units. For the protonation process, local M11-L gives the best results. All of the other functionals show significant deviations.

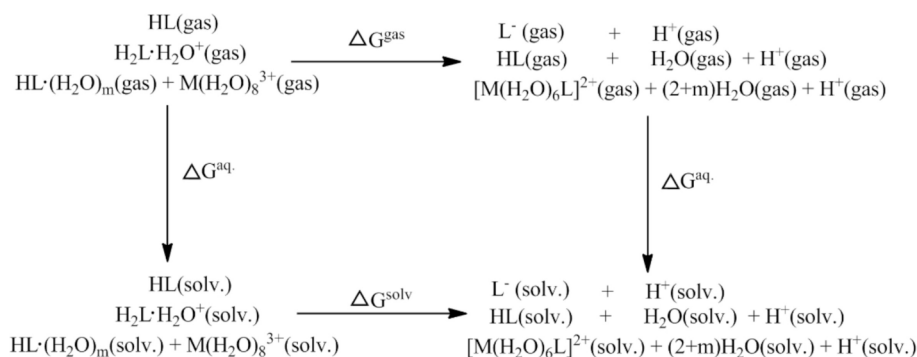
Currently, there are no suitable basis sets, which provide SCF-convergence for large lanthanide complexes with open-shell configuration. Assessments of chelation processes were performed for closed-shell metals only. Theoretically calculated values of formation constants and wavelengths of maximum absorbance are given in Table 4 (at level PBE0/SMD).

Aquacomplexes of REMs(III) exist in the form of $[M(H_2O)_n]^{3+}$, $n = 5$ –10. In this work, aquacomplex species of Sc³⁺, Y³⁺, La³⁺, and Lu³⁺ were approximated by $[M(H_2O)_8]^{3+}$ structures (Fig. S3). This approximation has proved its effectiveness for similar perfluorinated diketones, even for light lanthanides [51]. Structures of formed chelates were approximated by a six-membered chelate cycle: selenoyl-

Table 4

Theoretical parameters of complexation processes.

| Complex | m | $\Delta \Delta G$, kJ/mol | $\log K^{\text{calc}}$ | $\log K^{\text{exp}}$ | λ^{calc} , (nm) | λ^{exp} , (nm) |
|--------------|---|----------------------------|------------------------|-----------------------|--------------------------------|-------------------------------|
| Sc(III)-FBTA | 1 | -68.77 | 12.05 | 11.49 | 360 | 360 |
| Y(III)-FBTA | 2 | -38.55 | 6.75 | 5.61 | 353 | 355 |
| La(III)-FBTA | 2 | -21.70 | 3.80 | 4.87 | 353 | 356 |
| Lu(III)-FBTA | 3 | -27.47 | 4.81 | 5.50 | 357 | 355 |



Scheme 3. Thermodynamic cycle for DFT estimations.

Table 3

Theoretical values of dissociation and protonation constants.

| Dissociation process (cc-pVDZ) | | | | Protonation process (Def2-TZVP) | | | |
|--------------------------------|----------------------------|------------------------|-----------------------|---------------------------------|----------------------------|---------------------------------------|--------------------------------------|
| Density functional | $\Delta \Delta G$, kJ/mol | $\log K^{\text{calc}}$ | $\log K^{\text{exp}}$ | Density functional | $\Delta \Delta G$, kJ/mol | $-\text{p}K_{\text{a}}^{\text{calc}}$ | $-\text{p}K_{\text{a}}^{\text{exp}}$ |
| PBE0 | 43.30 | 7.58 | 6.40 | revTPSS | -5.57 | 0.98 | 1.85 |
| revTPSS | 35.10 | 6.15 | | PBE0 | -16.89 | -2.96 | |
| M06 | 37.36 | 6.54 | | B3LYP | -29.51 | 5.17 | |
| M06-2X | 35.86 | 6.28 | | BLYP | -25.60 | 4.48 | |
| B3LYP | 42.67 | 7.47 | | M06-HF | -61.28 | 10.74 | |
| BLYP | 37.43 | 6.56 | | M06-2X | -44.08 | 7.72 | |
| M06-HF | 26.13 | 4.58 | | M11-L | -11.90 | 2.08 | |

trifluoroacetone as a bidentate ligand and six water molecules (Fig. S3).

It's easy to see that for this model PBE0 functional provides the best results - predicted wavelengths are almost equal to the experimental data (Table 4). To achieve a good agreement between theory and experiment, the solvation forms of the ligand were used ($m = 1-3$, Scheme 3). Calculated values of stability constants ($\log K$) differ from experimental on 0.5–1.2 logarithmic units. The best value is observed for scandium(III), probably due to the use of the full-electron basis set. Theoretical and experimental values of stability constants are increased in the same series: $\text{La}^{+3} < \text{Lu}^{+3} < \text{Y}^{+3} < \text{Sc}^{+3}$.

4. Conclusion

A selenium-containing ligand – selenoyl-trifluoroacetone – has been synthesized and first characterized by various physicochemical methods. Acid-base properties were determined in aqueous solutions - in buffer and highly acidic media. The dissociation process was examined for three values of ionic strengths ($I = 0.25, 0.50, \text{ and } 1.00 \text{ M, NaCl}$) in the pH region 3.0–8.5.

Values of pK_a are between 6.3 and 6.5 logarithmic units. The protonation constant ($-\text{pK}_H$) is equal to 1.85 logarithmic units. These parameters are close to the analogous values for thenoyl- and furoyl-trifluoroacetone. Complexation characteristics were determined in glycine-HCl and acetate buffer media at $I = 0.5 \text{ M (NaCl)}$. First formation constants of monocomplex species with sixteen rare-earth metals range from 4.5 to 11.5 logarithmic units. Obtained constants non-monotonically decrease from Sc to Lu and high on 0.5–1 logarithmic unit than stability constants of REMs(III)-thenoyl- and furoyl-trifluoroacetone complexes. Complexes of Se- CF_3 can be divided into three groups: La-Nd, Sm-Tb, and Dy-Lu. The electrostatic interaction has been observed for the group of ‘heavy’ lanthanides (Dy-Lu) and, to a small extent, ‘light’ lanthanides (La-Nd). The correlation between stability constants and ionic potential is lack for complexes of Sm^{3+} , Eu^{3+} , Gd^{3+} , and Tb^{3+} , which may be related to spin-orbital interaction.

DFT assessments of keto-enol and spectral properties of selenoyl-trifluoroacetone have shown the predomination of keto-form. The cc-pVDZ/PBE0/SMD method demonstrate good convergence with experimental spectral properties for Se- CF_3 , as well as for other CF_3 -diketones. Thus, it can be recommended to predict spectral parameters for such type of ligands in aqueous solutions.

Acid-base parameters were successfully reproduced using M06-2X and M11-L density functionals for dissociation and protonation process, respectively. Parameters of the complex species were modeling by using a pseudopotential basis set CRENBL ECP (for Y^{+3} , La^{+3} , and Lu^{+3}) and full-electron cc-pVDZ (for Sc^{3+}). Chelation processes were approximated by using octa-coordinated aquacomplexes and $[\text{M}(\text{H}_2\text{O})_6\text{L}]^{2+}$ species. PBE0 functional gives correct results for describing spectral properties of complexes. Calculated values of $\log K$ are close to the experimental values of stability constant: difference $\log K^{\text{exp}} - \log K^{\text{calc}}$ is no more than 0.5–1.2 logarithmic units. Theoretical and experimental chelation parameters have the same order of increasing: $\text{La}^{+3} < \text{Lu}^{+3} < \text{Y}^{+3} < \text{Sc}^{+3}$.

Declaration of Competing Interest

The authors declare that they have no known competing financial interests or personal relationships that could have appeared to influence the work reported in this paper.

Acknowledgements

This work was conducted within the framework of the budget project # 0287-2021-0017 for Institute of Chemistry and Chemical Technology SB RAS using the equipment of Krasnoyarsk Regional Research Equipment Centre of SB RAS. Synthetic part of this work was financially supported by the Russian Science Foundation (Project N^o19-13-00272).

Numerical computations were performed on the MVS-1000M cluster of the Institute of computational modeling SB RAS.

Appendix A. Supplementary data

Supplementary data to this article can be found online at <https://doi.org/10.1016/j.poly.2021.115383>.

References

- [1] A.J. Brock, J.K. Clegg, F. Li, L.F. Lindoy, *Coord. Chem. Rev.* 375 (2018) 106–133.
- [2] J.K. Clegg, L.F. Lindoy, J.C. McMurtriea, D. Schilter, *Dalton Trans.* (2006) 3114–3121.
- [3] H. Wang, Z. Zhang, H. Wang, L. Guo, L. Lei, *Dalton Trans.* 48 (2019) 15970–15976.
- [4] S.M. Krajewski, A.S. Crossman, E.S. Akturk, T. Suhrbier, S.J. Scappaticci, M. W. Staab, M.P. Marshak, *Dalton Trans.* 48 (2019) 10714–10722.
- [5] K. Tanaka, Y. Chujo, *NPG Asia Mater.* 7 (2015), e223.
- [6] P.A. Vigato, V. Peruzzo, S. Tamburini, *Coord. Chem. Rev.* 253 (2009) 1099–1201.
- [7] J.J. Wilson, S.J. Lippard, *J. Med. Chem.* 55 (2012) 5326–5336.
- [8] K. Nakashima, F. Kubota, M. Goto, T. Maruyama, *Anal. Sci.* 25 (2009) 77–82.
- [9] A. Jyothi, G.N. Rao, *Proc. Indian Acad. Sci. (Chem. Sci.)* 100 (1988) 455–457.
- [10] A.-S. Chauvin, F. Gumy, I. Matsubayashi, Y. Hasegawa, J.-C.-G. Bünzli, *Eur. J. Inorg. Chem.* (2006) 473–480.
- [11] J. Alstad, J.H. Augustson, L. Farbu, *J. Inorg. Nucl. Chem.* 36 (1974) 899–903.
- [12] M.P. Jensen, M. Borkowski, I. Laszak, J.V. Beitz, P.G. Rickert, M.L. Dietz, *Sep. Sci. Technol.* 47 (2012) 233–243.
- [13] W. Cho, G. Sarada, H. Lee, M. Song, Y.-S. Gal, Y. Lee, S.-H. Jin, *Dyes Pigment.* 136 (2017) 390–397.
- [14] S.E. Livingstone, *Q. Rev. Chem. Soc.* 19 (1965) 386–425.
- [15] D. Das, P. Singh, M. Singh, A.K. Singh, *Dalton Trans.* 39 (2010) 10876–10882.
- [16] W.C. Wolsey, *J. Chem. Educ.* 50 (1973) A335–A337.
- [17] W.R. Robinson, *J. Chem. Educ.* 62 (1985), 1001–1001.
- [18] P. Linda, G. Marino, *J. Chem. Soc. B* (1970) 43–45.
- [19] Y.K. Yur'ev, N.N. Mezentsova, *J. Gen. Chem. USSR* 31 (1961) 1341–1353.
- [20] C.H. Gammons, S.T. Wood, Y. Li, *Environ. Geochem.* 7 (2002) 191–207.
- [21] D.J. Leggett (Ed.), *Computational Methods for the Determination of Formation Constants*, Springer US, Boston, MA, 1985.
- [22] M.A. Lutoshkin, N.N. Golovnev, *Heterocycl. Commun.* 22 (2016) 111–116.
- [23] R. Cox, K. Yates, *Can. J. Chem.* 61 (1983) 2225–2229.
- [24] R. Cox, K. Yates, *Can. J. Chem.* 59 (1981) 2023–2028.
- [25] S.A. Grebenyuk, I.F. Perepichka, A.F. Popov, *Spectrochim. Acta Part A Mol. Biomol. Spectrosc.* 58 (2002) 2913–2923.
- [26] A.I. Petrov, I.D. Dergachev, S.V. Trubina, S.B. Erenburg, M.A. Lutoshkin, N. N. Golovnev, A.A. Kondrasenko, V.D. Dergachev, *RSC Adv.* 4 (2014) 52384–52392.
- [27] <http://www.wolfram.com/>.
- [28] M.W. Schmidt, *Comput. Chem. (Oxford)* 14 (1993) 1347–1363.
- [29] C. Adamo, V. Barone, *J. Chem. Phys.* 110 (1999) 6158–6170.
- [30] S. Grimme, J. Antony, S. Ehrlich, H. Krieg, *J. Chem. Phys.* 132 (2010) 154104–154126.
- [31] J. Tirado-Rives, W.L. Jorgensen, *J. Chem. Theory Comput.* 4 (2008) 297–306.
- [32] J.P. Finley, *Mol. Phys.* 102 (2004) 627–639.
- [33] Y. Zhao, D.G. Truhlar, *Theor. Chem. Account* 120 (2008) 215–241.
- [34] J.P. Perdew, A. Ruzsinszky, G.I. Csonka, L.A. Constantin, *Phys. Rev. Lett.* 106 (2011), 179902.
- [35] T.H. Dunning Jr, *J. Chem. Phys.* 90 (1989) 1007–1023.
- [36] F. Weigend, R. Ahlrich, *PCCP* 7 (2005) 3297–3305.
- [37] B.P. Pritchard, D. Altaraw, B. Didier, T.D. Gibson, T.L. Windus, *J. Chem. Inf. Model.* 59 (2019) 4814–4820.
- [38] M.A. Lutoshkin, A.S. Kazachenko, *J. Comput. Methods Sci. Eng.* 17 (2017) 851–863.
- [39] V.S. Bryantsev, S.D. Mamadou, W.A. Goddard III, *J. Phys. Chem. B* 112 (2008) 9709–9719.
- [40] M.A. Lutoshkin, A.I. Petrov, N.N. Golovenov, *J. Sol. Chem.* 45 (2016) 1453–1467.
- [41] A.V. Marenich, C.J. Cramer, D.G. Truhlar, *J. Phys. Chem. B* 113 (2009) 6378–6396.
- [42] A.D. Laurent, D. Jacquemin, *Int. J. Quantum Chem.* 113 (2013) 2019–2039.
- [43] Y.Y. Rusakov, L.B. Krivdin, S.P.A. Sauer, E.P. Levanova, G.G. Levkovskaya, *Magn. Reson. Chem.* 48 (2010) 44–52.
- [44] B.A. Trofimov, E.Y. Schmidt, A.I. Mikhaleva, C. Pozo-Gonzalo, J.A. Pomposo, M. Salsamendi, N.I. Protzuk, N.V. Zorina, A.V. Afonin, A.V. Vashchenko, E. P. Levanova, G.G. Levkovskaya, *Chem. Eur. J.* 15 (2009) 6435–6445.
- [45] P. De Maria, A. Fontana, G. Siani, D. Spinelli, *EurJOC* 9 (1998) 1867–1872.
- [46] Selenophene anti-tumor agents. Chang, Ching-Jer; Ashendel, Curtis L.; Kim, Darrick, Patent WO9746225 (1997-12-11).
- [47] G.N. Dorofeenko, S.V. Krivun, V.I. Dulenko, Y.A. Zhdanov, *Russ. Chem. Rev.* 34 (1965) 88–104.
- [48] I.V. Taydakov, Y.M. Kreshchenova, E.P. Dolotova, *Beilstein J. Org. Chem.* 14 (2018) 3106–3111.
- [49] M.A. Lutoshkin, I.V. Taydakov, B.N. Kuznetsov, *J. Chem. Eng. Data* 64 (2019) 2593–2600.
- [50] M.A. Lutoshkin, Y.N. Malyar, *J. Chem. Eng. Data* 65 (2020) 3696–3705.
- [51] M.A. Lutoshkin, A.I. Petrov, Y.N. Malyar, A.S. Kazachenko, *Inorg. Chem.* 60 (2021) 3291–3304.
- [52] J. Stary, J.O. Liljenzin, *Pure Appl. Chem.* 54 (2009) 2557–2592.

- [53] C. Kremer, J. Torres, S. Domínguez, A. Mederos, *Coord. Chem. Rev.* 249 (2005) 567–590.
- [54] R.S. Kolat, J.E. Powell, *Inorg. Chem.* 1 (1962) 293–296.
- [55] P. Migal, N. Chebotar, A. Sorochinskaya, *Zhur. Neorg. Khim.* 16 (1971) 102–122.
- [56] E. Ohyoshi, *Anal. Chem.* 57 (1985) 446–448.
- [57] Y.Y. Yakubovich, V.G. Alekseev, *Russ. J. Inorg. Chem.* 57 (2012) 911–915.
- [58] S. Cotton, *Lanthanide and Actinide Chemistry*, John Wiley & Sons Ltd, The Atrium, Southern Gate, Chichester, 2006.
- [59] P. D'Angelo, A. Zitolo, V. Migliorati, G. Chillemi, M. Duvail, P. Vitorge, S. Abadie, R. Spezia, *Inorg. Chem.* 50 (2011) 4572–4579.
- [60] A.I. Petrov, M.A. Lutoshkin, I.V. Taydakov, *Eur. J. Inorg. Chem.* (2015) 1074–1082.
- [61] P.W. Atkins, A.J. MacDermott, *J. Chem. Educ.* 59 (1982) 359.